the plant journal

SEB SOCIETY FOR EXPERIMENTAL BIOLOGY

The Plant Journal (2024) doi: 10.1111/tpj.16618

The maize *PLASTID TERMINAL OXIDASE* (*PTOX*) locus controls the carotenoid content of kernels

Yongxin Nie[1,†], Hui Wang[2,†], Guan Zhang[3,†], Haiping Ding[1,†], Beibei Han[3], Lei Liu[4], Jian Shi[2], Jiyuan Du[1], Xiaohu Li[1], Xinzheng Li[1], Yajie Zhao[1], Xiaocong Zhang[5], Changlin Liu[5], Jianfeng Weng[5], Xinhai Li[5], Xiansheng Zhang[1], Xiangyu Zhao[1], Guangtang Pan[2], David Jackson[6], Qin-Bao Li[7], Philip S. Stinard[8], Jennifer Arp[9,10], Martin M. Sachs[8,9], Steven Moose[9], Charles T. Hunter[7], Qingyu Wu[3,*] and Zhiming Zhang[1,*]

[1]*State Key Laboratory of Crop Biology, College of Life Sciences, Shandong Agricultural University, Taian 271018, China,*
[2]*Maize Research Institute, Sichuan Agricultural University, Chengdu 611130, China,*
[3]*State Key Laboratory of Efficient Utilization of Arid and Semi-arid Arable Land in Northern China, the Institute of Agricultural Resources and Regional Planning, Chinese Academy of Agricultural Sciences, Beijing 100081, China,*
[4]*National Key Laboratory of Crop Genetic Improvement, Hubei Hongshan Laboratory, Huazhong Agricultural University, Wuhan 430070, China,*
[5]*Institute of Crop Sciences, Chinese Academy of Agricultural Sciences, Beijing 100081, China,*
[6]*Cold Spring Harbor Laboratory, Cold Spring Harbor, New York 11724, USA,*
[7]*USDA-ARS, Chemistry Research Unit, Gainesville, Florida 32608, USA,*
[8]*USDA-ARS, Maize Genetics Cooperation Stock Center, Urbana, Illinois 61801, USA,*
[9]*University of Illinois at Urbana-Champaign, Department of Crop Sciences, Urbana, Illinois 61801, USA, and*
[10]*Bayer Crop Science 700 Chesterfield Parkway West, Chesterfield, Missouri 63017, USA*

Received 20 March 2023; revised 16 December 2023; accepted 20 December 2023.
*For correspondence (e-mail zhzhang@sdau.edu.cn, wuqingyu@caas.cn)
†These authors contributed equally.

SUMMARY

Carotenoids perform a broad range of important functions in humans; therefore, carotenoid biofortification of maize (*Zea mays* L.), one of the most highly produced cereal crops worldwide, would have a global impact on human health. *PLASTID TERMINAL OXIDASE* (*PTOX*) genes play an important role in carotenoid metabolism; however, the possible function of *PTOX* in carotenoid biosynthesis in maize has not yet been explored. In this study, we characterized the maize *PTOX* locus by forward- and reverse-genetic analyses. While most higher plant species possess a single copy of the *PTOX* gene, maize carries two tandemly duplicated copies. Characterization of mutants revealed that disruption of either copy resulted in a carotenoid-deficient phenotype. We identified mutations in the *PTOX* genes as being causal of the classic maize mutant, *albescent1*. Remarkably, overexpression of *ZmPTOX1* significantly improved the content of carotenoids, especially β-carotene (provitamin A), which was increased by ~threefold, in maize kernels. Overall, our study shows that maize *PTOX* locus plays an important role in carotenoid biosynthesis in maize kernels and suggests that fine-tuning the expression of this gene could improve the nutritional value of cereal grains.

Keywords: carotene, provitamin A, biofortification, *albescent1*.

INTRODUCTION

The lack of certain micronutrients poses a serious threat to human health. This is particularly true in developing countries, where people predominantly subsist on cereal grains, which lack some important nutrients. For example, carotenoids, a group of yellow or red pigments with antioxidant activity, are essential for human health but are present at low levels in cereal grains. Therefore, carotenoid biofortification of major cereal crops used as food and feed worldwide would have a global impact on human health (Owens et al., 2014; Wurtzel et al., 2012).

In plants, carotenoids function as accessory pigments during light harvesting and structural components of the photosynthetic apparatus. They also serve as a precursor for numerous secondary metabolites and plant hormones such as abscisic acid (ABA) and strigolactones (Jia et al.,

2018; Nisar et al., 2015). The carotenoid metabolic pathway has been intensively studied in plants (reviewed by (Collini, 2019)). Carotenoids are synthesized in plastids from the colorless pigment phytoene via a series of sequential desaturation reactions. The first two desaturation reactions are catalyzed by phytoene desaturase (PDS), which results in the formation of phytofluene and then ζ-carotene (Bartley et al., 1991). The ζ-carotene is then catalyzed by ζ-carotene desaturase (ZDS) to form neurosporene and then lycopene (Albrecht et al., 1995). Lycopene is cyclized to form either α- or β-carotene, which can be oxidized to produce xanthophylls in photosynthetic tissues. PDS and ZDS require plastoquinone (PQ) as an electron-accepting cofactor (Norris et al., 1995) and PQ is maintained in an available (oxidized) state for these reactions by plastid terminal oxidase (PTOX) (Foudree et al., 2012; Joet et al., 2002; Kuntz, 2004). PTOX also serves to protect photosynthetic machinery during conditions of photo-oxidative stress (Cournac et al., 2002; Stepien & Johnson, 2018).

The first plant *PTOX* gene was identified in the *immutans* (*im*) mutant of *Arabidopsis thaliana* (Carol et al., 1999; Wu et al., 1999), which shows a variegated phenotype. Cells in green sectors of the *im* mutant possess normal-appearing chloroplasts, while cells in the white sectors lack carotenoid pigments and appear to be blocked at various stages of chloroplast biogenesis (Aluru et al., 2001; Wetzel et al., 1994; Yu et al., 2007). Orthologous mutants of *PTOX* in tomato (*Solanum lycopersicum* L.), are termed *ghost* mutants and have similar variegation in addition to pale or white immature fruit due to the lack of photo-protective carotenoids (Barr et al., 2004). Besides its function in carotenoid biosynthesis, PTOX also regulates plant architecture by affecting the biosynthesis of plant hormones. Rice (*Oryza sativa* L.) *ptox* mutants show variegation similar to *im* and *ghost* but also exhibit excessive tillering and semi-dwarfism, due to deficiency of strigolactones (Tamiru et al., 2014). *Chlamydomonas reinhardtii* possesses two isoforms of PTOX with, one of which appears to have a greater role in regenerating PQ for use by PDS while the other functions primarily during photosynthesis (Houille-Vernes et al., 2011).

Although the importance of *PTOX* genes for carotenoid metabolism, chloroplast function, and shoot architecture has been characterized in various plant species, the function of these genes in maize (*Zea mays* L.), the most produced cereal crop, has not yet been reported. Here, we identified the maize *PTOX* locus, containing two functional genes, by forward- and reverse-genetic approaches. Characterization of *Zmptox1* and *Zmptox2* mutants reveals an important role of the *PTOX* locus in carotenoid biosynthesis in maize leaves and kernels. We demonstrate that engineering this gene can enhance the carotenoid content and nutritional value of maize grains.

RESULTS

Map-based cloning of *ZmPTOX1*

To identify the key genes involved in carotenoid biosynthesis in maize kernels, we performed ethyl methanesulfonate (EMS) mutagenesis screening on the Chinese elite maize inbred line RP125 and searched for mutants with pale kernels, an indicator of low carotenoid accumulation in the endosperm (Nie et al., 2021). A mutant with much paler kernels than the wild type (RP125, yellowish kernels) was identified in the M2 population (Figure 1a). The mutants also displayed leaf variegation, with white and green sectors, at the seedling stage (Figure 1b) and accumulated less chlorophyll than the wild-type plants (Figure 1c). Together, these results suggest that the mutants exhibit not only low carotenoid accumulation but also abnormal chloroplast biogenesis.

To identify and clone the causal gene, we generated a recombinant F2 population by crossing the recessive mutant with B73 inbred line and performed bulked segregant analysis (BSA) using pooled RNA samples representing approximately 30 mutant or wild-type kernels (Gallavotti & Whipple, 2015). We mapped the gene to an approximately 2 Mb region on the short arm of chromosome 2. Using ~850 individual mutants, we narrowed down the region to ~100 kb containing two putative genes in the B73 reference genome v4, *Zm00001d001909* (hereafter *ZmPTOX1*) and *Zm00001d001908* (hereafter Zm*PTOX2*). Gene models indicate multiple transcript variants for both genes at this locus. The most recent gene models for B73 (Zm0001eb066920 from B73-REFERENCE-NAM-5.0 [B73v5]) have four transcript variants for Zm*PTOX1* with variations in splicing of the third, fourth, and fifth exons. We sequenced full-length cDNAs and confirmed the presence of two transcript variants for *ZmPTOX1*, matching T001 and T004 from Zm0001eb066920 (Figure 2; Supplementary Data S1). Gene models for Zm*PTOX2* are more complex and appear to incorrectly include multiple independent genes in some cases. In B73v5 (Zm00001eb066910) there are two variants with differences restricted to the 3′ end. Our sequencing of cDNAs of *ZmPTOX2* provided evidence for two transcripts (T01 and T02) with 86.9% identified with *ZmPTOX1* (Figure 2; Supplementary data S1).

Sequencing the *PTOX* locus of the EMS mutant revealed a G-to-A mutation in the exon 5 of Zm00001d001909, which was predicted to change the tryptophan residue at position 186 to a premature stop codon (Figure 1d). We also identified two additional mutants, with phenotypes like Zmptox1-1, in our EMS collection (Figure 1e; Supplementary Figure S1a). Both alleles carried mutations at splice sites in Zm00001d001909, leading to incorrectly spliced transcripts. The mutation on the splicing site of *Zmptox1-2* introduced a 36-bp deletion within the transcript leading to a 12 AA deletion on the alternative

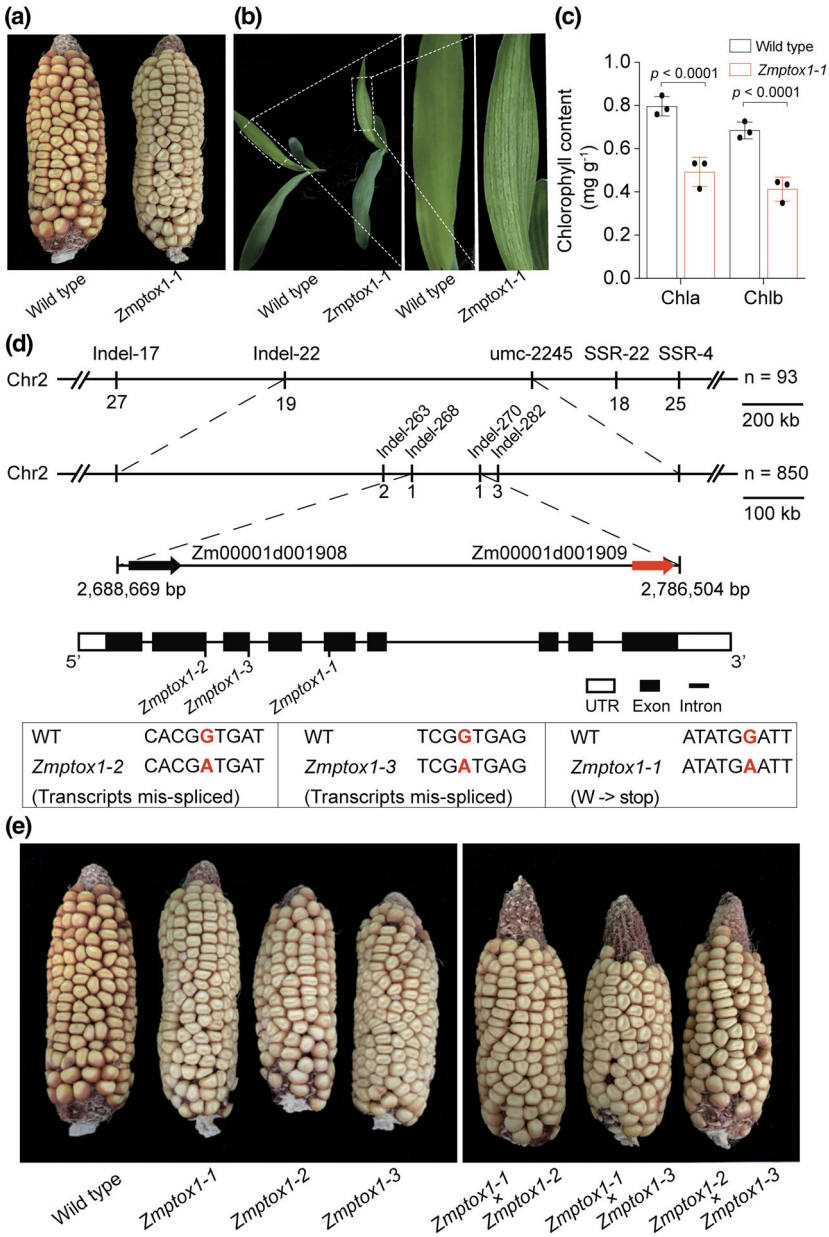

Figure 1. Map-based cloning of *ZmPTOX1* (a) Ear phenotypes of the wild-type (RP125) and *Zmptox1* mutants. The kernels of mutants are paler than those of the wild type.
(b) Leaf phenotype of wild-type and *Zmptox1* mutant plants. The leaves of mutants are paler than those of the wild type.
(c) Chlorophyll content of the *Zmptox1* mutant was significantly lower than that of the wild type.
(d) Scheme for positional cloning of the *Zmptox1* gene.
(e) Comparison of the ear phenotypes of allelic mutants and their progenies with that of the wild type.

oxidase (AOX) domain, which is critical to the biochemical function of *PTOX* (Supplementary Figure S1b,c). The mutation on the splicing site of *Zmptox1-3* caused a 128-bp intron retention and introduced a premature stop codon (Figure 1d; Supplementary Figure S1b,d). The F1 plants obtained by crossing these mutants displayed similar phenotypes (Figure 1e), confirming that the two mutants were allelic and that the mutations in Zm00001d001909 were responsible for the pale phenotype of kernels.

To further validate the association between the disruption of ZmPTOX1 and the phenotype, we sought additional UniformMu Mutator transposon alleles of *Zmptox1* from the Maize Genetics Cooperation Stock Center (McCarty et al., 2013; Settles et al., 2007). Three transposon insertions were

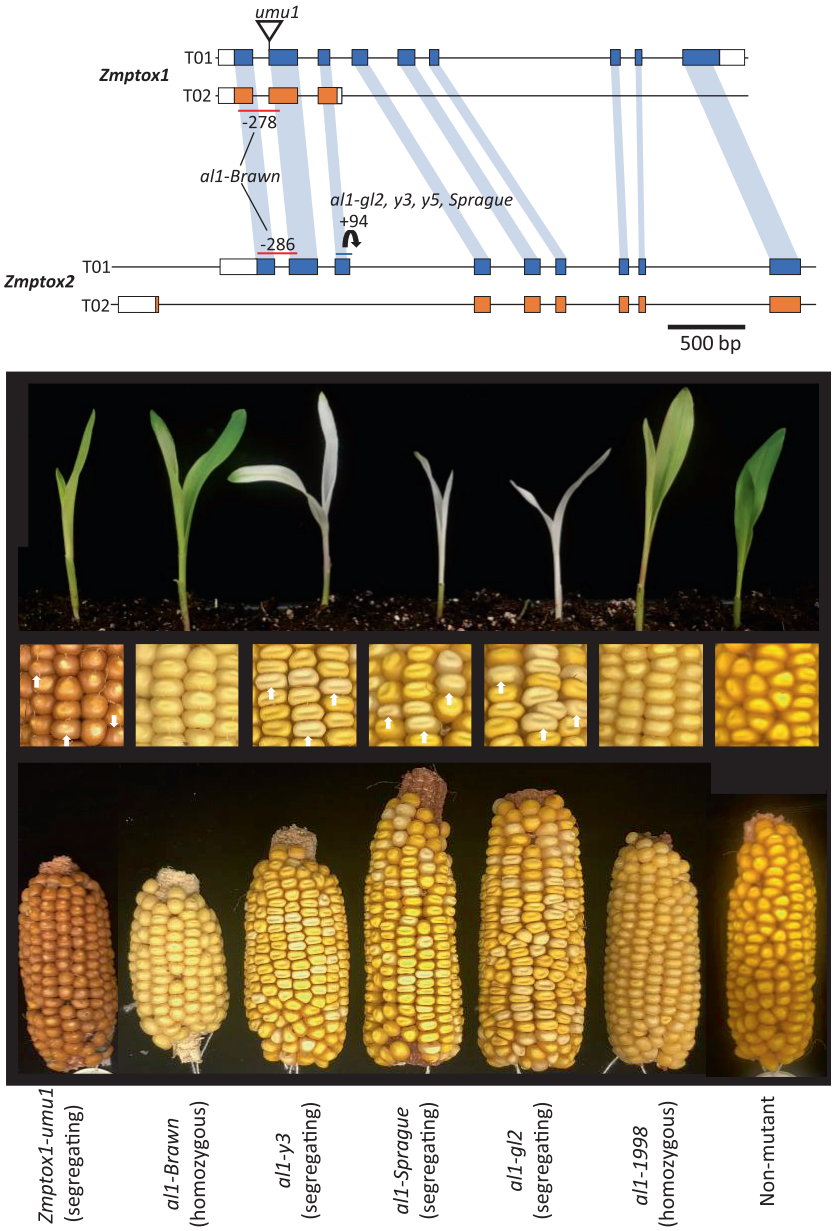

Figure 2. Additional mutations identified in *Zmptox1* and *Zmptox2*. Two UniformMu transposon insertions were identified in *Zmptox1*. The *Zmptox1-umu1* allele at the intron/exon border of the second intron co-segregated with pale kernels that germinated into seedlings with pale leaves. An allelic series of *albescent1* (*al1*) mutants was analyzed for changes to the *Zmptox1* and *Zmptox2* genes. The *al1-Brawn* allele contained similar deletions in both *Zmptox1* and *Zmptox2* resulting in a 62 amino acid in-frame deletion in *Zmptox1* and a frameshift mutation in *Zmptox2*. The *al1-gl2-ref*, *al1-y3*, *al1-y5*, and *al1-Sprague* alleles all contained the same 94-base tandem duplication of exon 3 in *ptox2*. The duplication is retained in the *ZmPTOX2* mRNA and introduces a premature stop codon. This *al1* mutant contains intact, full-length transcript for *Zmptox1*. The *al1-1998* allele did not contain mutations that would be predicted to disrupt the translation of either *Zmptox1* or *Zmptox2*.

identified in *Zmptox1* (Figure 2). The *Zmptox1-umu1* (mu1034172) insertion occurred across the intron-exon border at the 5′ end of exon 2 and co-segregated with pale kernels that germinated into seedlings with pale leaves. These plants were able to grow to maturity and produced ears with uniformly pale kernels.

The classic maize mutant *albescent1* (*al1*) is characterized by pale kernels that germinate into seedlings having pale or sectored leaves and maps close by the *Zmptox* locus (Stinard, 2014). We obtained an allelic series of *al1* mutants and conducted Sanger sequencing of PCR-amplified *ZmPTOX1* and *ZmPTOX2* genomic DNA and cDNA from *al1* mutant seedlings to test association between the *al1* phenotype and *ZmPTOX* (Supplemental data 1). We found that *al1-gl2-ref*, *al1-y3*, *al1-y5*, and *al1-Sprague* all contained a 94-base tandem duplication of

exon 7 in *ZmPTOX2* that would introduce a premature stop codon (Figure 2). These alleles all contained full-length, intact transcripts for *ZmPTOX1*. The *al1-Brawn* mutant contained deletions in both *ZmPTOX1* (278 bp deletion that causes a − 186 bp in-frame deletion within the mRNA leading to a 62 AA deletion) and *ZmPTOX2* (286 bp deletion that would disrupt the reading frame) (Figure 2). The fact that the leaf color varies between these alleles is likely due to the variable penetrance of these mutants in different genetic backgrounds.

ZmPTOX1 regulates carotenoid biosynthesis in maize kernels

Protein BLAST and phylogenetic analysis revealed that *Zm00001d001909* encodes PTOX (Figure 3a), an enzyme that activates the plastid enzyme PDS, which in turn converts the colorless phytoene to ζ-carotene, a precursor of colored carotenoids (Wetzel et al., 1994 and Figure 3b). PTOX acts to maintain oxidized PQ to serve as a cofactor of PDS and ZDS, two enzymes required for carotenoid biosynthesis. To determine whether this mechanism is conserved in maize kernels, we examined the activities of PDS and ZDS in wild-type and *Zmptox1-1* kernels. Both enzymes showed reduced activity in mutant kernels compared with wild-type kernels (Figure 3c,d), suggesting that ZmPTOX1 participates in carotenoid biosynthesis by regulating the activity of PDS and ZDS via control of available PQ9.

To confirm whether the pale color of mutant kernels was indeed caused by the lower accumulation of colored carotenoids, we measured the contents of colored carotenoids, including lutein, zeaxanthin, and carotene, as well as that of phytoene in wild-type and mutant kernels. The mutant kernels accumulated more noncolored pigments such as phytoene (Figure 3e) and fewer colored pigments such as lutein and zeaxanthin (Figure 3f,g). Additionally, neither α-carotene nor β-carotene was detected in mutant kernels. These results confirmed that the pale color of mutant kernels resulted from impairment of carotenoid biosynthesis due to the disruption of *ZmPTOX1*.

To gain further insights into the transcriptomic changes in *Zmptox1* mutant kernels, we performed RNA-seq analyses on wild-type and *Zmptox1-1* mutant kernels sampled at 9, 12, and 20 days postpollination (dpp) Principal component analysis (PCA) showed a strong correlation among the biological replicates of each genotype, indicating that our RNA-seq data were highly reliable (Supplementary Figure S2a). Comparison between the RNA-seq data of *Zmptox1* and wild-type kernels led to the detection of 1523 (905 upregulated and 618 downregulated), 571 (283 upregulated and 288 downregulated), and 523 (277 upregulated and 246 downregulated) differentially expressed genes (DEGs) at 9, 12, and 20 dpp, respectively (Supplementary Table S1). A total of 26 DEGs were significantly upregulated, and 26 DEGs were downregulated, at least at one time point (Supplementary Figure S2b,c). Functional enrichment analysis of the DEGs using the Kyoto Encyclopedia of Genes and Genomes (KEGG) database revealed 20 representative pathways at three developmental stages (Figure 4a), among which the 'plant-pathogen interaction pathway' was the most highly enriched, suggesting that either PTOX functions in pathogen resistance or changes in carotenoid metabolism affect pathogen fitness. A closer look at the transcriptomes revealed that the expression of genes involved in methylerythritol phosphate (MEP), mevalonate (MVA), and carotenoid pathways remained largely unchanged in *ptox1* mutant kernels compared with wild-type kernels (Figure 4b).

Phenotypes associated with the disruption of *PTOX* have been reported in other plant species such as Arabidopsis, tomato, and rice; however, these phenotypes were related only to changes in leaf color, fruit color, and shoot architecture and not to changes in seed color (Barr et al., 2004; Carol et al., 1999; Tamiru et al., 2014; Wu et al., 1999). Additionally, Arabidopsis, tomato, and rice possess only one copy of *PTOX*, whereas maize has two tandemly duplicated *PTOX* genes separated by ~80 kb (Figure 3a). *ZmPTOX1* transcripts were more abundant than *ZmPTOX2* transcripts (Figure 4d), consistent with a previous study (Walley et al., 2016), which could explain why the impairment of *ZmPTOX1* alone was sufficient to cause pale kernels and variegated leaves. Indeed, the expression of *ZmPTOX2* was unchanged in *Zmptox1* mutants, not upregulated so as to complement the *ZmPTOX1* deficiency (Figure 4c).

To determine whether natural variation in *ZmPTOX1* is associated with carotenoid content, we conducted a candidate gene association study using a maize association panel (n = 368 diverse inbred lines) and previously published carotenoid content data (Fu et al., 2013). The results revealed four single nucleotide polymorphisms (SNPs) and one InDel in *ZmPTOX1*, all of which showed significant association with carotenoid content. Three SNPs (2.2779620 T>C, 2.2779776 A>C, 2.2779998 A>G) were associated with α-carotene content, while the remaining one SNP (2.2778989 C>T) and one InDel (2.2778979 TTTTC>T) in the promoter region of *ZmPTOX1* were associated with the lutein content of kernels (Figure 5a). Among the three α-carotene content-associated SNPs, two were found in the intron and one in the exon (2 779 620 bp). The exonic SNP was nonsynonymous and predicted to cause proline-to-serine amino acid substitution. Consistent with our finding, *ZmPTOX1* was also found to be associated with the carotenoid content of maize kernels in a separate GWAS study that was conducted using the US nested association mapping panel (Diepenbrock et al., 2021). Overall, our findings showed that natural variation in *ZmPTOX1* influences

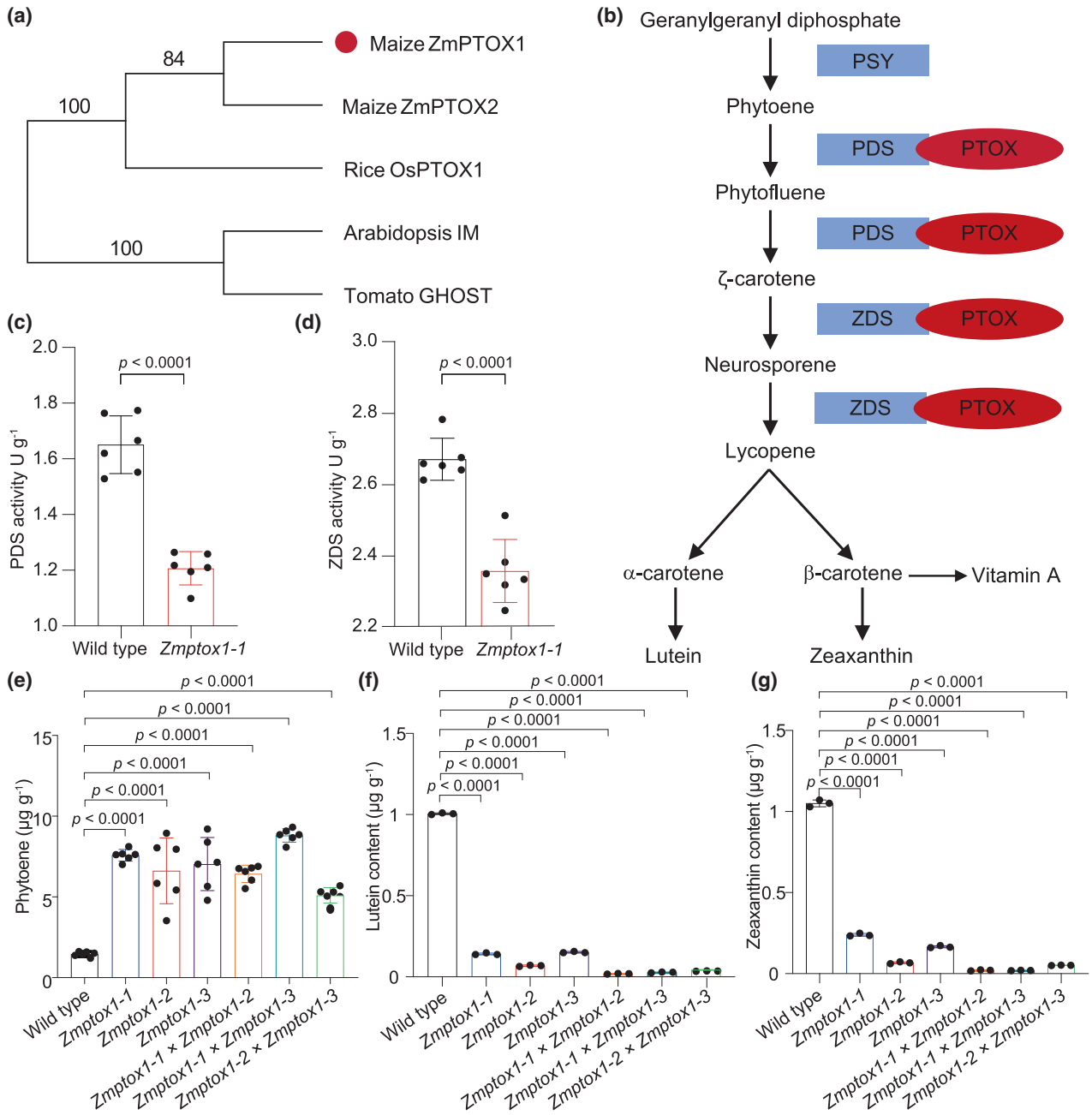

Figure 3. *ZmPTOX1* regulates carotenoid biosynthesis in maize kernels.
(a) Phylogenetic analysis of *PTOX* genes of maize, rice, Arabidopsis, and tomato.
(b) Biosynthetic pathway of lutein and zeaxanthin.
(c, d) Activities of PDS (c) and ZDS (d) in *Zmptox1* mutants and wild-type (RP125) plants.
(e–g) Contents of phytoene (e), lutein (f), and zeaxanthin (g) in wild-type and *Zmptox1* kernels.

lutein and α-carotene contents (Figure 5b,c; Supplemental Table S3), suggesting that the manipulation of this gene may enhance the carotenoid content of maize kernels.

A previous study showed that maize represents, on average, only 57.1% of the nucleotide diversity in teosinte (Wright et al., 2005). To determine whether *ZmPTOX1* underwent selection during maize domestication and improvement, we calculated the nucleotide diversity of *ZmPTOX1* in improved maize lines, landraces, and teosinte using HapMap 3 (Bukowski et al., 2017). Nucleotide diversity was high in teosinte but significantly reduced in the improved maize lines, especially in the region highlighted in red in Figure 5d ($\pi_{Maize}/\pi_{Teosinte}$ = 15%). Furthermore, coalescent simulations incorporated the demographic

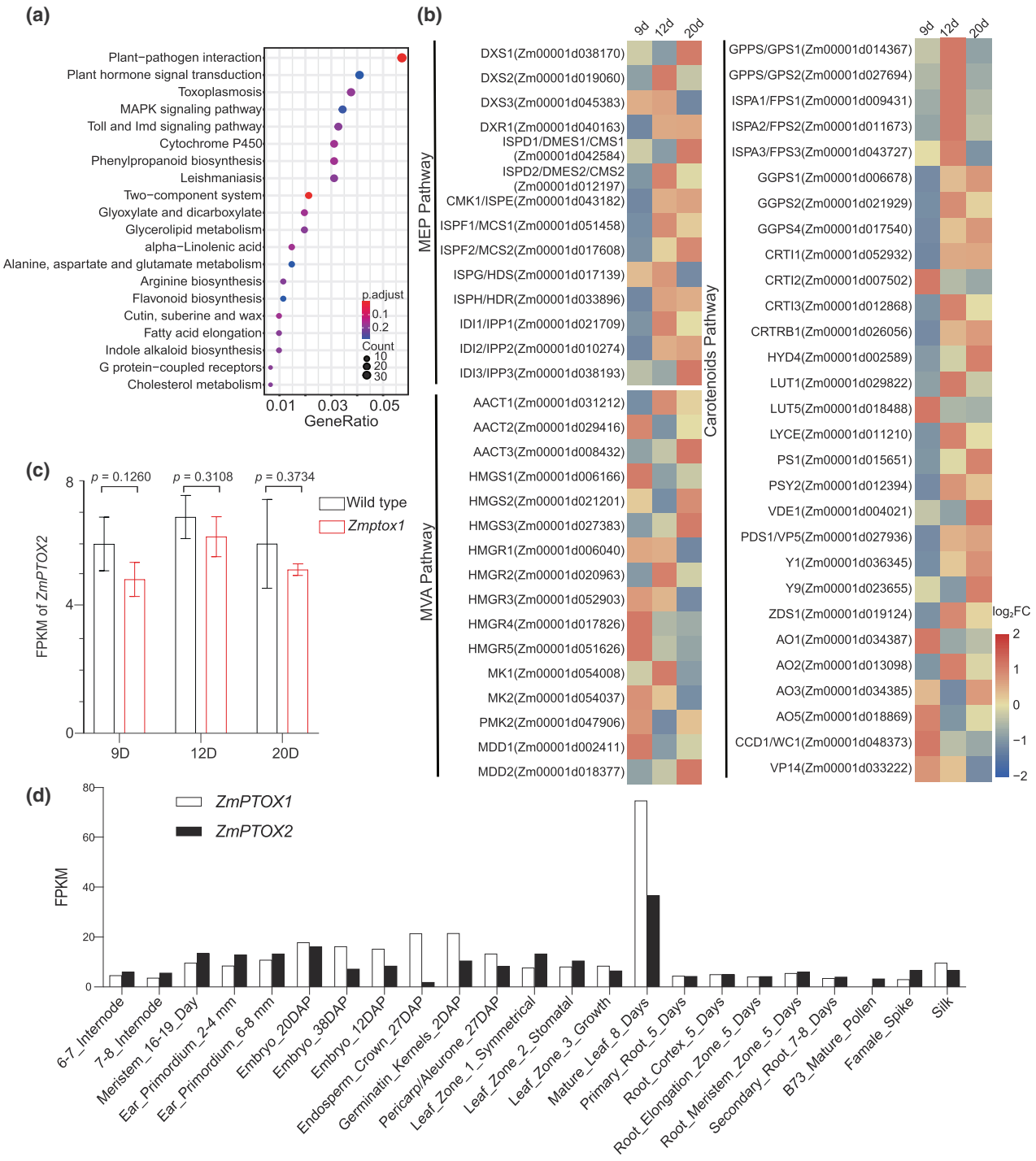

Figure 4. Transcript profiling of wild-type and *Zmptox1* mutant kernels at 9, 12, and 20 dpp.
(a) KEGG enrichment of DEGs.
(b) Comparison of the expression levels of MEP, MVP, and carotenoid pathway genes in wild-type controls and *Zmptox1* mutants.
(c, d) Expression levels of *ZmPTOX1* and *ZmPTOX2* in mutant and wild-type kernels (c) and other tissues (d).

history of maize domestication and $\pi_{Teosinte}/\pi_{Maize}$ >2.98 ($P < 0.01$) showed a significant deviation from the neutral expectation. These data suggest that *ZmPTOX1* underwent positive selection throughout the maize domestication process; however, the implication of this selection remains to be explored.

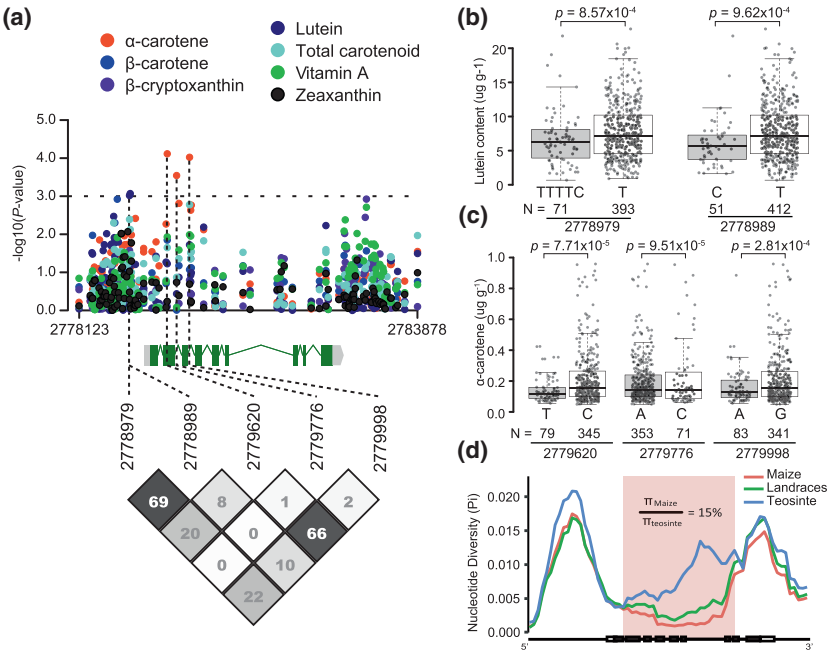

Figure 5. Natural variation in the promoter and open reading frame (ORF) of *ZmPTOX1* is associated with the pale color of maize kernels.
(a) Two SNPs in the promoter and three SNPs in the ORF of *ZmPTOX1* show association with lutein and α-carotene contents, respectively. The dashed line indicates the threshold of significant association ($P \leq 0.001$). The numbers show the pairwise linkage disequilibrium pattern by R^2 (%). The positions of five significant SNPs are shown on the top of the pairwise linkage disequilibrium plot and indicated by dashed lines in the gene diagram.
(b, c) The contents of lutein and α-carotene are associated with SNPs in diverse inbred lines. Each box represents the median and interquartile range, and whiskers extend to maximum and minimum values. The genotype and number (N) of each allele are listed below each box.
(d) Evidence of selection pressure on *ZmPTOX1*. The red area shows low nucleotide diversity in improved maize lines compared with teosinte, as analyzed using maize HapMap v3 SNP data. Red, green, and blue lines represent the nucleotide diversity of improved maize lines, landraces, and teosinte, respectively. White and black rectangles on the *x*-axis represent the untranslated regions (UTRs) and exons of the *ZmPTOX1* gene.

Overexpression of Zm*PTOX1* improves nutritional content of maize kernels

To determine whether *ZmPTOX1* could directly enhance the nutritional content of maize kernels, we overexpressed *ZmPTOX1* under the control of the maize ubiquitin promoter. Ten independent events were obtained, three of which were randomly selected for further analysis. Quantitative real-time PCR (qRT-PCR) revealed that *ZmPTOX1* was upregulated 10–45-fold in all three overexpression (OE) lines relative to the wild-type controls (Figure 6a). Additionally, the levels of lutein, zeaxanthin, and α-carotene were nearly twofold greater, and the levels of the β-carotene were threefold higher, in transgenic kernels than in wild-type controls (Figure 6b–e). We also examined the activities of PDS and ZDS in B104 and OE-2. Both enzymes showed slightly increased activity in OE line (Supplementary Figure S3a,b). However, we did not observe a significant increase in *ZmPSY1* expression in OE lines (Supplementary Figure S3c), suggesting that *ZmPTOX* does not regulate *PSY1* at the transcriptional level. These findings demonstrate that manipulating *ZmPTOX1* expression is effective in improving maize carotenoid content.

DISCUSSION

Through forward genetic screening, we identified a *PTOX* gene in maize, one of the most important cereal crops worldwide, and demonstrated that engineering this gene dramatically increases the levels of carotenoids, particularly β-carotene, a nutrient crucial for human health. The carotenoid biosynthetic pathway in plants has been established through the cloning and characterization of genes using specific carotenoid mutants. Although phytoene synthase (PSY), which is responsible for phytoene biosynthesis, has received much attention as a rate-limiting enzyme in this pathway (Chayut et al., 2017; Zhou et al., 2015), the PDS and ZDS enzymes, which desaturate phytoene and ζ-carotene, are also critical for the biosynthesis of downstream health-promoting carotenoids (McQuinn et al). In tomato, PDS becomes limiting once PSY1 is elevated during fruit ripening (McQuinn et al., 2018). Thus, new bottlenecks emerge in subsequent desaturation steps to promote the activity of PDS and ZDS. Our data show that PTOX is a promising target for engineering maize cultivars with high carotenoid content.

Although the maize genome carries two tandemly duplicated *PTOX* genes, in contrast to the single *PTOX*

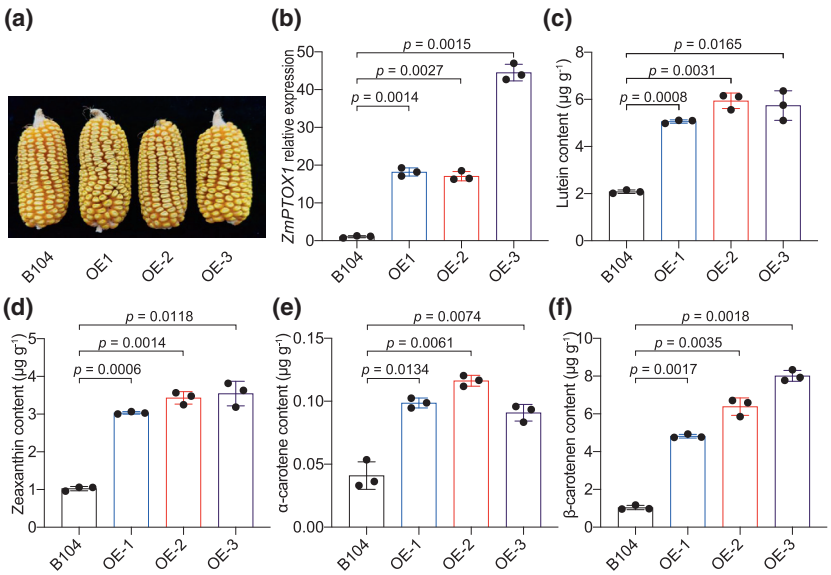

Figure 6. Characteristics of three Zm*PTOX1*-overexpressing maize lines (OE1–3).
(a) Ears of wild-type (B104), OE1, OE2, and OE3 plants.
(b) *ZmPTOX1* transcripts were more abundant in the transgenic lines.
(c–f) Overexpression of *ZmPTOX1* increased the contents of lutein (c), zeaxanthin (d), α-carotene (e), and β-carotene (f).
In (b–f), data represent mean ± standard deviation (SD; $n = 3$). Significant differences were determined using Student's *t*-test. Raw data are plotted in the bar charts.

gene in Arabidopsis, tomato, and rice, disrupting one of the two copies in maize is sufficient to impair carotenoid biosynthesis in grains. *PTOX* exists as a single-copy gene in most plant species (Barr et al., 2004; Carol et al., 1999; Tamiru et al., 2014; Wu et al., 1999); however, in some cyanobacteria and algae, two copies of the *PTOX* gene have been reported (Houille-Vernes et al., 2011; Wang et al., 2009), of which one copy is more important than the other. For example, *Chlamydomonas* has *PTOX1* and *PTOX2*; however, PTOX2 is the predominant enzyme isoform involved in chlororespiration, and the *ptox2* single mutant shows lower fitness than the wildtype when grown under phototrophic conditions (Houille-Vernes et al., 2011). Our study is the first describing a higher plant containing two copies of *PTOX*, and that disrupting one copy is sufficient to cause obvious phenotypes. Although both *ZmPTOX1* and *ZmPTOX2* were expressed in a variety of tissues, *ZmPTOX1* transcripts were more abundant than *ZmPTOX2* transcripts in the majority of maize tissues (Figure 4d; Walley et al., 2016), particularly mature leaves and endosperm, which showed clear changes in color because of decreased pigment accumulation (Figures 1a,c and 2h). Our findings imply that *ZmPTOX1* plays a major role in carotenoid biosynthesis, and its disruption is sufficient to impair this process. However, whether the maize *PTOX* genes exhibit a dosage effect remains to be explored. Elevating the abundance of *ZmPTOX1* transcripts increased downstream carotenoid abundance, indicating that dosage effect is likely (Figure 5). However, detailed characterization of *Zmptox1* and *Zmptox2* single and double mutants in the same genetic background is required before drawing firm conclusions.

In addition to chloroplast biogenesis and carotenoid biosynthesis, PTOXs are also potentially involved in other physiological processes such as stress tolerance and plant development (Johnson & Stepien, 2016; Tamiru et al., 2014). For example, transgenic tobacco plants transformed with the *PTOX1* gene of the green alga *Chlamydomonas reinhardtii* outperformed wild-type controls in terms of seed germination rate, root length, and shoot biomass accumulation under high NaCl concentrations. Transgenic tobacco plants also displayed better recovery and less chlorophyll bleaching than wild-type plants after the NaCl treatment (Ahmad et al., 2020). Rice *ptox* mutants displayed excessive tillering and a semidwarf phenotype, demonstrating the importance of PTOX in strigolactone biosynthesis (Tamiru et al., 2014). However, the *Zmptox1* mutants did not exhibit obvious developmental phenotypes compared with wild-type plants. One explanation is that the two *ZmPTOX* genes in maize perform redundant functions; thus, *ZmPTOX2* can compensate for the loss of function of *ZmPTOX1* and is adequate to sustain the biosynthesis of strigolactones in the *Zmptox1* mutant. To verify whether *ZmPTOX1* and *ZmPTOX2* are redundant genes, double mutants are needed. Given the diverse functions of PTOXs in regulating carotenoid biosynthesis, plant development, and stress resistance, fine-tuning the expression of *ZmPTOX1* has potential to both improve the nutritional value and enhance the stress tolerance of maize.

EXPERIMENTAL PROCEDURES

Identification and map-based cloning of the *ZmPTOX1* gene

To identify the *PTOX* gene in maize, pollen (2 ml) of the RP125 inbred line (wildtype) was treated with 0.066% EMS (Sigma-Aldrich, M0880, Saint Louis, MO, USA) solution in mineral oil (Sigma-Aldrich, M8410) for 30 min. The mutagenized pollen was

then used to pollinate the ears of RP125. The F2 segregating population was constructed by crossing the M2 *Zmptox1* mutants in the RP125 background with B73. RNA was extracted from ~30 pooled normal or mutant seeds, and BSA-seq was performed as described previously (Gallavotti & Whipple, 2015). Candidate genes in the mapping region were amplified from the mutants and subjected to Sanger sequencing. The deduced amino acid sequences of these candidate genes were aligned using the MUSCLE model, and a phylogenetic tree was constructed using the neighbor-joining method in MEGA7 with 1000 bootstrap replicates (Kumar et al., 2016).

The UniformMu alleles in *ZmPTOX1*, mu1034172 (*ptox1-umu1*) in UFMu-03227, and the classic *albescent1* (*al1*) alleles, *al1-gl2-ref*, *al1-Brawn*, *al1-y3*, *al1-Sprague*, and *al1-1998*, were obtained from the Maize Genetic Cooperation Stock Center. The UniformMu families were analyzed for the presence of the transposons in *ZmPTOX1* by PCR using gene-specific primers along with a *Mutator*-specific terminal inverted repeat primer TIR6 Mutant leaf samples from the *al1* alleles were sampled for genomic DNA and RNA. cDNA was made using the SuperScript IV First-Strand Synthesis System (Invitrogen, Cat. 18 091 050, Shanghai, China). Transcript-specific primers were used to amplify cDNAs from normal and mutant leaf samples to identify transcript variants and possible causal mutations. Genomic and cDNA sequences were amplified using gene-specific primers and sequenced using Sanger sequencing. Conditions for all PCR reactions followed protocols from Phusion high-fidelity DNA polymerase (NEB, Cat. M0530L, Shanghai, China). See Supplemental Table S2 for primer sequences.

Overexpression lines

The *ZmPTOX1* overexpression vector was constructed by cloning the coding region of *ZmPTOX1* under the control of the maize ubiquitin promoter. The construct was transformed into *Agrobacterium*, which was then used to transform the maize inbred line B104 as described previously (Frame et al., 2015).

Carotenoid analysis

The carotenoid extraction method described for alfalfa (*Medicago truncatula*) (Meng et al., 2019) was used in this study, with minor modifications. Seeds of the following genotypes were used for carotenoid extraction: wildtype, *Zmptox1-1*, *Zmptox1-2*, *Zmptox1-3*, B104, and OE lines. Briefly, the dissected maize tissues (30 mg) were ground into powder in liquid nitrogen. Then, 200 μl of 6% (w/v) KOH (in methanol) was added to the ground tissue. The samples were vortexed for 10 sec and heated at 60°C for 1 h in the dark. Subsequently, 200 μl of 50 mM HCl buffer (pH 7.5, containing 1 M NaCl) was added to each sample. Samples were allowed to cool to room temperature in the dark, thoroughly mixed by turning the tubes upside-down eight to ten times, and then incubated on ice for 10 min. Then, 800 μl of chloroform was added to the sample, mixed by inverting eight to ten times and incubated on ice for 10 min. The mixtures were centrifuged at 3000 × ***g*** for 5 min at 4°C. Then, the lower liquid phase (600 μl) was removed and again extracted using 800 μl of chloroform. The two chloroform extracts were combined, dried with a blowing device using high-quality nitrogen, and then dissolved in 100 ml of ethyl acetate. The different pigments were identified by high-performance liquid chromatography (HPLC; A30).

HPLC analysis was performed on seed as described previously (Fraser et al., 2000), with minor modifications. Briefly, a C30 column at 30 ± 1°C was used with solvent A (methanol, methyl cyanide, water, and butylated hydroxytoluene) and solvent B (methyl tert-butyl ether) as mobile phases, with a flow rate of 1.0 ml/min flow rate and an injection volume of 10 μl. Carotenoids were identified by comparing their absorption spectra and retention period with those of the standards. The contents of carotenoids were calculated using standards.

The activities of PDS, ZDS, and PSY enzymes were determined using the ELISA-based method (LMAI Bio, Shanghai, China), according to the manufacturer's instructions. Solid-phase plant-purified anti-PDS, -ZDS, and -PSY antibodies were used to coat microtiter plate wells. Then, PDS, ZDS, and PSY enzymes were added to the wells. An antibody–antigen–enzyme–antibody complex was labeled with combined antibodies and horse radish peroxidase (HRP). After thorough washing, the reaction was stopped by adding sulfuric acid, which turns the TMB substrate blue when catalyzed by HRP. The color change was then measured spectrophotometrically at a wavelength of 450 nm. The optical density (OD) of the samples was then compared with the standard curve to determine the PDS, ZDS, and PSY concentrations in the samples.

RNA-seq and data analysis

Kernels of wild-type and *Zmptox1* mutant plants were harvested at 9, 12, and 20 days postpollination (dpp), with three biological replicates at each time point. Total RNA was extracted from the kernels using the TRIzol reagent, as directed by the manufacturer. The sequencing libraries were produced with the Illumina TruSeq RNA Sample Prep Kit and sequenced on the Illumina HiSeq X Ten System. The quality of raw sequence reads was checked using Fastp v.0.12.4 (Chen et al., 2018). HISAT2 v.2.2.1, with default settings, was used to map the clean reads to the maize B73 RefGen_V4 reference genome sequence (Kim et al., 2015). StringTie v.2.0.4 was utilized to calculate gene expression levels as fragments per kilobase of transcript per million reads (FPKM) (Pertea et al., 2016). DEGs were identified using DESeq2 based on two criteria: log2fold-change ≥1 and adjusted *P*-value cutoff ≤0.05 (Love et al., 2014).

Candidate gene association and nucleotide diversity analyses

Candidate gene association analysis was conducted using a maize association panel of 368 diverse inbred lines. *ZmPTOX1*-specific SNPs and InDels were downloaded from previous sequence data (Gui et al., 2022) and metabolite content data of the members of this panel were downloaded from the previously released genotype dataset (Fu et al., 2013). Association between metabolite contents and *ZmPTOX1*-specific SNPs and InDels (MAF > 0.05) was determined using a mixed linear model, after correction for familial relatedness and population structure, with a *P*-value of 0.001 as a threshold (Je et al., 2018). The third-generation haplotype map data of *Zea mays* were downloaded. Nucleotide diversity was investigated in improved maize lines, landraces, and teosinte using vcftools (https://vcftools.github.io/examples.html), with a 1 kb window and 100 bp step along the 2 kb upstream and 1 kb downstream regions of *ZmPTOX1*, respectively. coalescent simulations following the demographic history of maize domestication were performed using Ms program, with parameters as previously described, and running 10 000 coalescent simulations (Huang et al., 2018; Tian et al., 2009).

ACKNOWLEDGEMENTS

Funding for this work was provided by the National Natural Science Foundation of China (32171925, U21A20210) to Q.W.; The National Key Research and Development Program of China (2022YFD1201703), Taishan Scholars Program of Shandong Province (tsqn201909074), and Shandong Natural Science Foundation

(ZR2020KC019) to Z.Z.; The Agricultural Science and Technology Innovation Program (GJ2023-14-11 and GJ2023-14-5) and Fundamental Research Funds for Central Non-profit Scientific Institution (G2023-01-30) to Q.W.; Key R&D Program of Shandong Province (2021LZGC022-2) to H.D.; Shandong Natural Science Foundation (ZR2022MC076) to Y.N.; National Science Foundation (NSF) to DJ (IOS-2129189); and United States Department of Agriculture, Agricultural Research Service research project 6036-21000-011-00D to C.H. USDA is an equal opportunity provider and employer. We thank Prof. Junjie Fu and Dr. Jie Zhang for their advice on nucleotide diversity analyses.

AUTHOR CONTRIBUTIONS

QW, ZZ, YN, HW, GZ, HD, DJ, GP, XYZ, XSZ, JA, SM, CH, and XHL designed research and wrote the paper. YN, HW, GZ, and HD cloned the *ZmPTOX1* gene. JS, JD, XL, XZL, YZ, XZ, CL, JW, GPZQ, KZ, QL, YC, CZ, CL, JW, XL, XSZ, XYZ, GP, BH, QL, JA, MS, SM, CH LL, and DJ performed candidate gene association analysis.

CONFLICT OF INTEREST

The authors declare no competing interest.

DATA AVAILABILITY STATEMENT

The raw data are available from Zhiming Zhang or Qingyu Wu upon request. All RNA-seq datasets reported in this study have been deposited in GenBank (NCBI) with the following accession code: PRJNA943556.

SUPPORTING INFORMATION

Additional Supporting Information may be found in the online version of this article.

Data S1. The full sequences for *Zmptox1* and *Zmptox2* variants from the maize stock center.

Figure S1. (a) Comparison of the leaf phenotype of *Zmptox1* mutants with that of the wild type. (b, c, d) Alignment of *ZmPTOX1-2, ZmPTOX1-3*, and wild-type alleles.

Figure S2. Statistics of DEGs. (a) Principal component analysis (PCA) of transcriptome data. (b) Venn diagram of upregulated DEGs at 9, 12, and 20 days after pollination. (c) Venn diagram of downregulated DEGs at 9, 12, and 20 days after pollination.

Figure S3. (a, b) Activities of PDS (a) and ZDS (b) in overexpression line and wild-type (B104) plants. (c) The expression of *ZmPSY1* in overexpression lines and wild-type (B104) plants.

Table S1. The list of differentially expressed genes.

Table S2. The list of primers in this paper.

Table S3. The detailed information of *ZmPTOX1* association analysis.

REFERENCES

Ahmad, N., **Khan, M.O.**, **Islam, E.**, **Wei, Z.Y.**, **McAusland, L.**, **Lawson, T.** ***et al.*** (2020) Contrasting responses to stress displayed by tobacco overexpressing an algal plastid terminal oxidase in the chloroplast. *Frontiers in Plant Science*, **11**, 51.

Albrecht, M., **Klein, A.**, **Hugueney, P.**, **Sandmann, G.** & **Kuntz, M.** (1995) Molecular-cloning and functional expression in Escherichia-Coli of a novel plant enzyme mediating zeta-carotene desaturation. *FEBS Letters*, **372**, 199–202.

Aluru, M.R., **Bae, H.**, **Wu, D.Y.** & **Rodermel, S.R.** (2001) The Arabidopsis immutans mutation affects plastid differentiation and the morphogenesis of white and green sectors in variegated plants. *Plant Physiology*, **127**, 67–77.

Barr, J., **White, W.S.**, **Chen, L.**, **Bae, H.** & **Rodermel, S.** (2004) The GHOST terminal oxidase regulates developmental programming in tomato fruit. *Plant Cell and Environment*, **27**, 840–852.

Bartley, G.E., **Viitanen, P.V.**, **Pecker, I.**, **Chamovitz, D.**, **Hirschberg, J.** & **Scolnik, P.A.** (1991) Molecular cloning and expression in photosynthetic bacteria of a soybean cDNA coding for phytoene desaturase, an enzyme of the carotenoid biosynthesis pathway. *Proceedings of the National Academy of Sciences, USA*, **88**, 6532–6536.

Bukowski, R., **Guo, X.S.**, **Lu, Y.L.**, **Zou, C.**, **He, B.**, **Rong, Z.Q.** ***et al.*** (2017) Construction of the third-generation *Zea mays* haplotype map. *GigaScience*, **7**, 1–12.

Carol, P., **Stevenson, D.**, **Bisanz, C.**, **Breitenbach, J.**, **Sandmann, G.**, **Mache, R.** ***et al.*** (1999) Mutations in the Arabidopsis gene immutans cause a variegated phenotype by inactivating a chloroplast terminal oxidase associated with phytoene desaturation. *Plant Cell*, **11**, 57–68.

Chayut, N., **Yuan, H.**, **Ohali, S.**, **Meir, A.**, **Sa'ar, U.**, **Tzuri, G.** ***et al.*** (2017) Distinct mechanisms of the ORANGE protein in controlling carotenoid flux. *Plant Physiology*, **173**, 376–389.

Chen, S., **Zhou, Y.**, **Chen, Y.** & **Gu, J.** (2018) Fastp: an ultra-fast all-in-one FASTQ preprocessor. *Bioinformatics*, **34**, i884–i890.

Collini, E. (2019) Carotenoids in photosynthesis: the revenge of the "accessory" pigments. *Chem*, **5**, 494–495.

Cournac, L., **Latouche, G.**, **Cerovic, Z.**, **Redding, K.**, **Ravenel, J.** & **Peltier, G.** (2002) In vivo interactions between photosynthesis, mitorespiration, and chlororespiration in Chlamydomonas reinhardtii. *Plant Physiology*, **129**, 1921–1928.

Diepenbrock, C.H., **Ilut, D.C.**, **Magallanes-Lundback, M.**, **Kandianis, C.B.**, **Lipka, A.E.**, **Bradbury, P.J.** ***et al.*** (2021) Eleven biosynthetic genes explain the majority of natural variation in carotenoid levels in maize grain. *Plant Cell*, **33**, 882–900.

Foudree, A., **Putarjunan, A.**, **Kambakam, S.**, **Nolan, T.**, **Fussell, J.**, **Pogorelko, G.** ***et al.*** (2012) The mechanism of variegation in immutans provides insight into chloroplast biogenesis. *Frontiers in Plant Science*, **3**, 260.

Frame, B., **Warnberg, K.**, **Main, M.** & **Wang, K.** (2015) Maize (*Zea mays* L.). In: Wang, K. (Ed.) *Agrobacterium protocols. Methods in molecular biology*. New York, NY: Springer, pp. 101–117.

Fraser, P.D., **Pinto, M.E.**, **Holloway, D.E.** & **Bramley, P.M.** (2000) Technical advance: application of high-performance liquid chromatography with photodiode array detection to the metabolic profiling of plant isoprenoids. *The Plant Journal*, **24**, 551–558.

Fu, J.J., **Cheng, Y.B.**, **Linghu, J.J.**, **Yang, X.H.**, **Kang, L.**, **Zhang, Z.X.** ***et al.*** (2013) RNA sequencing reveals the complex regulatory network in the maize kernel. *Nature Communications*, **4**, 1038.

Gallavotti, A. & **Whipple, C.J.** (2015) Positional cloning in maize (*Zea mays* subsp *mays, Poaceae*). *Applications in Plant Sciences*, **3**, 1400092.

Gui, S., **Wei, W.**, **Jiang, C.**, **Luo, J.**, **Chen, L.**, **Wu, S.** ***et al.*** (2022) A pan-Zea genome map for enhancing maize improvement. *Genome Biology*, **23**, 178.

Houille-Vernes, L., **Rappaport, F.**, **Wollman, F.A.**, **Alric, J.** & **Johnson, X.** (2011) Plastid terminal oxidase 2 (PTOX2) is the major oxidase involved in chlororespiration in Chlamydomonas. *Proceedings of the National Academy of Sciences of the United States of America*, **108**, 20820–20825.

Huang, C., **Sun, H.**, **Xu, D.**, **Chen, Q.**, **Liang, Y.**, **Wang, X.** ***et al.*** (2018) ZmCCT9 enhances maize adaptation to higher latitudes. *Proceedings of the National Academy of Sciences of the United States of America*, **115**, E334–E341.

Je, B.I., **Xu, F.**, **Wu, Q.Y.**, **Liu, L.**, **Meeley, R.**, **Gallagher, J.P.** ***et al.*** (2018) The CLAVATA receptor FASCIATED EAR2 responds to distinct CLE peptides by signaling through two downstream effectors. *eLife*, **7**, e35673.

Jia, K.P., **Baz, L.** & **Al-Babili, S.** (2018) From carotenoids to strigolactones. *Journal of Experimental Botany*, **69**, 2189–2204.

Joet, T., **Genty, B.**, **Josse, E.M.**, **Kuntz, M.**, **Cournac, L.** & **Peltier, G.** (2002) Involvement of a plastid terminal oxidase in plastoquinone oxidation as evidenced by expression of the Arabidopsis thaliana enzyme in tobacco. *The Journal of Biological Chemistry*, **277**, 31623–31630.

Johnson, G.N. & **Stepien, P.** (2016) Plastid terminal oxidase as a route to improving plant stress tolerance: known knowns and known unknowns. *Plant and Cell Physiology*, **57**, 1387–1396.

Kim, D., **Langmead, B.** & **Salzberg, S.L.** (2015) HISAT: a fast spliced aligner with low memory requirements. *Nature Methods*, **12**, 357–360.

Kumar, S., **Stecher, G.** & **Tamura, K.** (2016) MEGA7: molecular evolutionary genetics analysis version 7.0 for bigger datasets. *Molecular Biology and Evolution*, **33**, 1870–1874.

Kuntz, M. (2004) Plastid terminal oxidase and its biological significance. *Planta*, **218**, 896–899.

Love, M.I., **Huber, W.** & **Anders, S.** (2014) Moderated estimation of fold change and dispersion for RNA-seq data with DESeq2. *Genome Biology*, **15**, 550.

McCarty, D.R., **Latshaw, S.**, **Wu, S.**, **Suzuki, M.**, **Hunter, C.T.**, **Avigne, W.T.** ***et al.*** (2013) Mu-seq: sequence-based mapping and identification of transposon induced mutations. *PLoS One*, **8**, e77172.

McQuinn, R.P., **Wong, B.** & **Giovannoni, J.J.** (2018) AtPDS overexpression in tomato: exposing unique patterns of carotenoid self-regulation and an alternative strategy for the enhancement of fruit carotenoid content. *Plant Biotechnology Journal*, **16**, 482–494.

Meng, Y., **Wang, Z.**, **Wang, Y.**, **Wang, C.**, **Zhu, B.**, **Liu, H.** ***et al.*** (2019) The MYB activator WHITE PETAL1 associates with MtTT8 and MtWD40-1 to regulate carotenoid-derived flower pigmentation in Medicago truncatula. *Plant Cell*, **31**, 2751–2767.

Nie, S.J., **Wang, B.**, **Ding, H.P.**, **Lin, H.J.**, **Zhang, L.**, **Li, Q.G.** ***et al.*** (2021) Genome assembly of the Chinese maize elite inbred line RP125 and its EMS mutant collection provide new resources for maize genetics research and crop improvement. *The Plant Journal*, **108**, 40–54.

Nisar, N., **Li, L.**, **Lu, S.**, **Khin, N.C.** & **Pogson, B.J.** (2015) Carotenoid metabolism in plants. *Molecular Plant*, **8**, 68–82.

Norris, S.R., **Barrette, T.R.** & **DellaPenna, D.** (1995) Genetic dissection of carotenoid synthesis in arabidopsis defines plastoquinone as an essential component of phytoene desaturation. *Plant Cell*, **7**, 2139–2149.

Owens, B.F., **Lipka, A.E.**, **Magallanes-Lundback, M.**, **Tiede, T.**, **Diepenbrock, C.H.**, **Kandianis, C.B.** ***et al.*** (2014) A foundation for provitamin a Biofortification of maize: genome-wide association and genomic prediction models of carotenoid levels. *Genetics*, **198**, 1699–1716.

Pertea, M., **Kim, D.**, **Pertea, G.M.**, **Leek, J.T.** & **Salzberg, S.L.** (2016) Transcript-level expression analysis of RNA-seq experiments with HISAT, StringTie and Ballgown. *Nature Protocols*, **11**, 1650–1667.

Settles, A.M., **Holding, D.R.**, **Tan, B.C.**, **Latshaw, S.P.**, **Liu, J.**, **Suzuki, M.** ***et al.*** (2007) Sequence-indexed mutations in maize using the UniformMu transposon-tagging population. *BMC Genomics*, **8**, 116.

Stepien, P. & **Johnson, G.N.** (2018) Plastid terminal oxidase requires translocation to the grana stacks to act as a sink for electron transport. *Proceedings of the National Academy of Sciences of the United States of America*, **115**, 9634–9639.

Stinard, P. (2014) A dominant enhancer of yellow color in albescent1 mutant endosperms identified in South American orange flint lines. *Maize Genetics Cooperation Newsletter*, **88**, 17.

Tamiru, M., **Abe, A.**, **Utsushi, H.**, **Yoshida, K.**, **Takagi, H.**, **Fujisaki, K.** ***et al.*** (2014) The tillering phenotype of the rice plastid terminal oxidase (PTOX) loss-of-function mutant is associated with strigolactone deficiency. *New Phytologist*, **202**, 116–131.

Tian, F., **Stevens, N.M.** & **Buckler, E.S.** (2009) Tracking footprints of maize domestication and evidence for a massive selective sweep on chromosome 10. *Proceedings of the National Academy of Sciences of the United States of America*, **106**(Suppl 1), 9979–9986.

Walley, J.W., **Sartor, R.C.**, **Shen, Z.X.**, **Schmitz, R.J.**, **Wu, K.J.**, **Urich, M.A.** ***et al.*** (2016) Integration of omic networks in a developmental atlas of maize. *Science*, **353**, 814–818.

Wang, J.X., **Sommerfeld, M.** & **Hu, Q.** (2009) Occurrence and environmental stress responses of two plastid terminal oxidases in Haematococcus pluvialis (Chlorophyceae). *Planta*, **230**, 191–203.

Wetzel, C., **Jiang, C.**, **Meehan, L.**, **Voytas, D.F.** & **Rodermel, S.** (1994) Nuclear—organelle interactions: the immutans variegation mutant of Arabidopsis is plastid autonomous and impaired in carotenoid biosynthesis. *The Plant Journal*, **6**, 161–175.

Wright, S.I., **Bi, I.V.**, **Schroeder, S.G.**, **Yamasaki, M.**, **Doebley, J.F.**, **McMullen, M.D.** ***et al.*** (2005) The effects of artificial selection on the maize genome. *Science*, **308**, 1310–1314.

Wu, D.Y., **Wright, D.A.**, **Wetzel, C.**, **Voytas, D.F.** & **Rodermel, S.** (1999) The immutans variegation locus of Arabidopsis defines a mitochondrial alternative oxidase homolog that functions during early chloroplast biogenesis. *Plant Cell*, **11**, 43–55.

Wurtzel, E.T., **Cuttriss, A.** & **Vallabhaneni, R.** (2012) Maize provitamin a carotenoids, current resources, and future metabolic engineering challenges. *Frontiers in Plant Science*, **3**, 29.

Yu, F., **Fu, A.G.**, **Aluru, M.**, **Park, S.**, **Xu, Y.**, **Liu, H.Y.** ***et al.*** (2007) Variegation mutants and mechanisms of chloroplast biogenesis. *Plant Cell and Environment*, **30**, 350–365.

Zhou, X.J., **Welsch, R.**, **Yang, Y.**, **Alvarez, D.**, **Riediger, M.**, **Yuan, H.** ***et al.*** (2015) Arabidopsis OR proteins are the major posttranscriptional regulators of phytoene synthase in controlling carotenoid biosynthesis. *Proceedings of the National Academy of Sciences of the United States of America*, **112**, 3558–3563.